ELSEVIER

Journal of Photochemistry and Photobiology A: Chemistry 147 (2002) 199–204

Journal of Photochemistry and Photobiology A:Chemistry

www.elsevier.com/locate/jphotochem

Radical-mediated photoreduction of manganese(II) species in UV-irradiated titania suspensions

Y. Ming, C.R. Chenthamarakshan, K. Rajeshwar*

Department of Chemistry and Biochemistry, The University of Texas at Arlington, Box 19065, Arlington, TX 76019-0065, USA

Received 18 July 2001; received in revised form 19 October 2001; accepted 19 October 2001

Abstract

New data are reported on the radical-mediated photoreduction of Mn(II) species in UV-irradiated TiO_2 suspensions. The influence of organic co-additives on the fate of Mn(II) ions in these media is the major focus of this study. It is also shown that some of these co-additives (formate, acetate or oxalate) induce the initial adsorption of Mn^{2+} ions on the TiO_2 particle surfaces in the dark. The influence of co-additive level, suspension pH, and TiO_2 particle dose on the photoreduction kinetics, is described. Experiments seeking the product identity and general conclusions that can be made from this study are finally presented.

Keywords: Heterogeneous photocatalysis; Adsorption; Organic co-additives

1. Introduction

Heterogeneous photocatalytic reactions in aqueous titania (TiO_2) suspensions have been extensively studied in recent years [1–7]. The vast majority of these studies, however, have focused on organic substrates. The photocatalytic reduction of metal ions with rather negative standard reduction potentials is of interest from both fundamental and practical (environmental remediation) perspectives. Thus, we [7–11] and others [12–14] have studied the reactivity of Zn^{2+} ($E^0 = -0.763$ V), Cd^{2+} ($E^0 = -0.40$ V), Pb^{2+} ($E^0 = -0.126$ V), Ni^{2+} ($E^0 = -0.257$ V), and Tl^{+} ($E^0 = -0.336$ V) in UV-irradiated TiO_2 suspensions (all potentials quoted in this study are with reference to the standard hydrogen electrode, SHE).

In this paper, we describe new findings on another metal ion, namely Mn(II), which is characterized by a rather negative standard reduction potential of -1.18 V (Fig. 1). While reports exist for the photocatalytic *oxidation* of Mn(II) in UV-irradiated TiO_2 suspensions [15–17], we are not aware of prior studies on the reductive reaction pathway. We show below that facile photoreduction of Mn^{2+} can be secured with suitable co-additives in the TiO_2 suspensions. Interesting dark adsorption patterns are also presented for Mn^{2+} in the presence of various organic co-additives.

2. Experimental

Manganese sulfate (99.999%, Alfa Aesar) was used without further purification; all other chemicals were of reagent grade. The TiO_2 (Degussa, P-25) photocatalyst was predominantly anatase and had a specific surface area of $\sim 60\ m^2\ g^{-1}$. Deionized water was used in all cases for making solutions or suspensions. The TiO_2 suspension dose was $2\ g\ l^{-1}$ unless otherwise specified.

The photoreactor used was described previously [12]. Briefly, an immersion-well design was employed with a double-walled jacket for lamp cooling. The light source was a 400 W medium-pressure Hg arc lamp (Philips). The TiO_2 suspensions were agitated by sparging ultrapure N_2 through them.

Prior to UV-irradiation, the Mn(II)-loaded TiO_2 suspensions were equilibrated in the dark for 30 min. The difference between the initial concentration of Mn(II) (200 μM unless otherwise specified) and the concentration at the end of the equilibration period was taken as the amount adsorbed on the TiO_2 particle surface in the dark. After this equilibration, the UV lamp was turned on and aliquots were syringed out periodically during irradiation. The solutions were analyzed for Mn(II) ions after removing TiO_2 particles using PTFE syringe filters.

A colorimetric procedure was used for the estimation of Mn(II) concentrations [18]. 4-(2-pyridylazo)-resorcinol (PAR) was used as the colorimetric reagent. In a typical procedure, 1 ml of Mn(II) sample was pipetted into a 25 ml volumetric flask, followed by addition of 1 ml of PAR

* Corresponding author. Tel.: +1-817-272-3810; fax: +1-817-272-3808.
E-mail address: rajeshwar@uta.edu (K. Rajeshwar).

1010-6030/02/$ – see front matter
PII: S1010-6030(01)00624-4

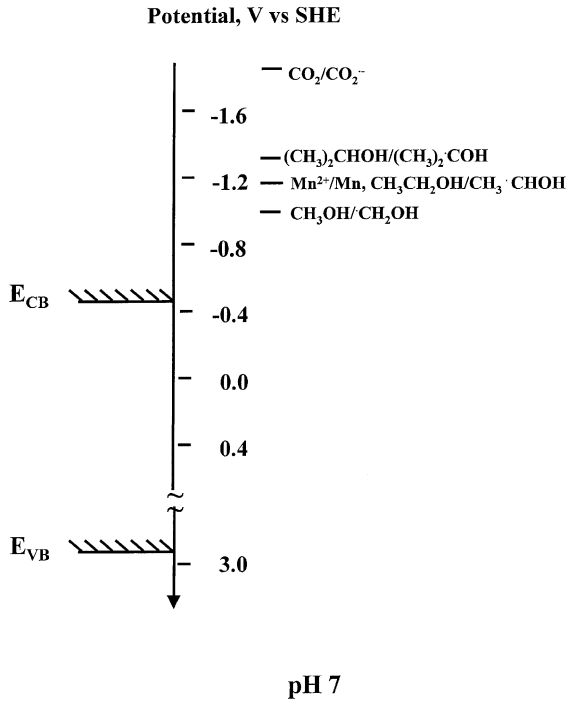

Fig. 1. Relative positions of the conduction and valence band edges for TiO_2 (pH 7 suspension) and related solution redox levels. Redox potentials involving the alcohols are from [22].

solution (0.05%, w/v), and dilution with distilled water to about 15 ml. Then 5 ml borax buffer (pH 10) solution was added and the total volume was brought to 25 ml after mixing the solution thoroughly. The Mn(II)–PAR complex concentrations were determined at $\lambda = 494$ nm from the Beer's law plot constructed from standard solutions.

UV–visible spectra were recorded on a Hewlett-Packard model HP 8452 diode array spectrometer. X-ray photoelectron spectroscopy (XPS) was performed on a Perkin-Elmer/Physical Electronics model 5000C system. The samples after photocatalysis were cast on microscopic glass plates for XPS analyses. Flame atomic absorption spectroscopy (FAAS) was performed on a Perkin-Elmer 2380 atomic absorption spectrometer using analytical wavelengths of 324.8 and 279.5 nm for copper and manganese, respectively.

The initial pH of the suspensions was between 6 and 7 unless otherwise noted. In experiments exploring the influence of pH (see Section 3.3 below), either HCl or NaOH was used to adjust the suspension pH to a targeted value in the 2–9 range.

3. Results and discussion

3.1. Dark adsorption of Mn(II) on the surface of TiO_2 and the influence of organic co-additives

In aqueous suspensions of pH∼7, Mn^{2+} ions exhibit little proclivity to adsorb on the TiO_2 particle surface in the dark.

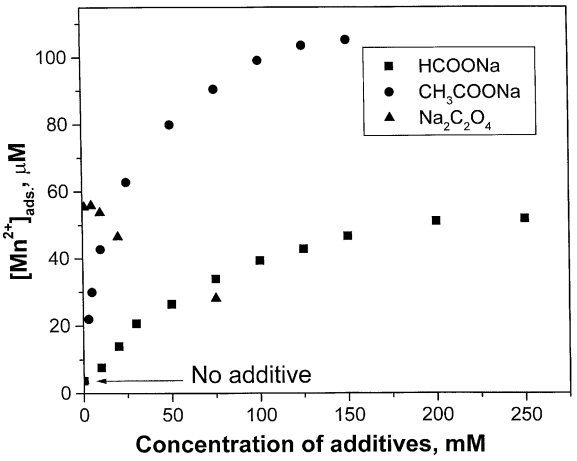

Fig. 2. Dependence of amount of Mn^{2+} adsorbed on the TiO_2 surface on the amount of organic co-additives.

This trend is in agreement with that observed by previous authors [19]. Fig. 2 contains plots of the amount of Mn^{2+} adsorbed versus the concentration of these organic co-additives utilized as the sodium salts. The ordinate values were computed from the difference between the initial Mn^{2+} concentration (200 μM) and that measured after 30 min equilibration (with the TiO_2 suspension) in the dark. Interestingly, both the monodentate species (HCOONa and CH_3COONa) induce a monotonic increase in the bound Mn^{2+} levels with the co-additive concentration (Fig. 2). On the other hand, the bidentate oxalate co-additive exhibits a very different trend: an initial very rapid increase followed by a monotonic decay in the amount of adsorbed Mn^{2+} species.

It is worth noting that adsorption behavior of the sort shown in Fig. 2 is rather unusual in the photocatalysis or TiO_2 surface chemistry literature. Namely, the dark adsorption of Mn^{2+} on the TiO_2 surface is *induced* by the presence of an organic co-additive. It is tempting to attribute this induced adsorption to an interfacial chelation effect (exerted by the organic ligands that themselves are bound to the TiO_2 surface) as we have done before for the Zn^{2+}, Cd^{2+}, and Tl^{+} cases [8–10]. Further mechanistic studies are underway to unravel these interfacial aspects, which however, are beyond the scope of the present study. In these ongoing experiments, we try to understand why acetate induces a twofold higher extent of adsorption than formate and why oxalate induces a markedly different interfacial profile (Fig. 2). Contrasting with these co-additives, three alcohol co-additives did not significantly perturb the negligible intrinsic adsorption of Mn^{2+} on the TiO_2 surface (Fig. 3).

3.2. Influence of organic co-additives on the photocatalytic reduction of Mn(II)

Fig. 3 contains data on the six organic co-additives along with the control experiment ($UV + TiO_2 + Mn^{2+}$). In interpreting these data (and those in Figs. 4–6 that follow), the

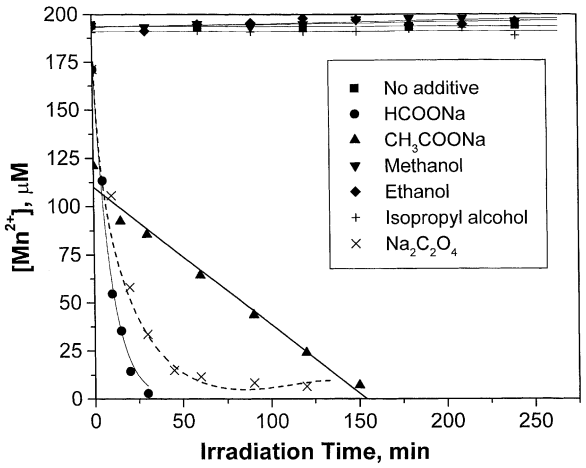

Fig. 3. Effect of organic co-additives (each at 0.05 M) on the photoreduction of Mn^{2+} ions.

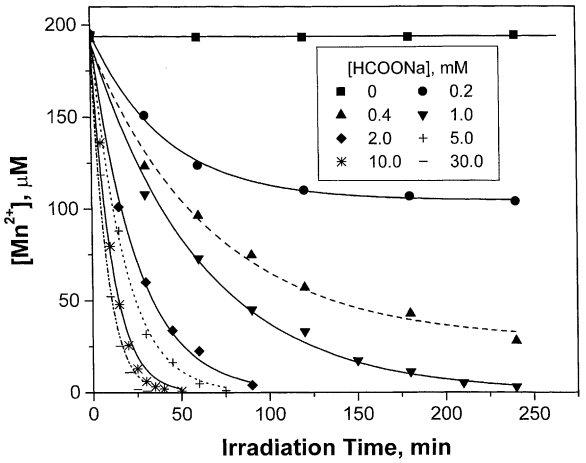

Fig. 4. Effect of HCOONa co-additive concentration on the photoreduction of Mn^{2+} ions.

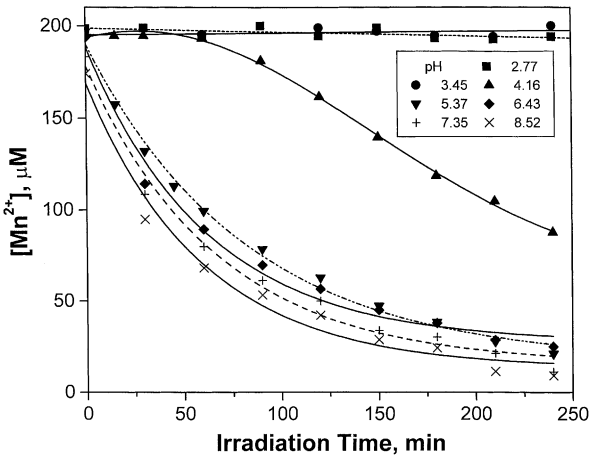

Fig. 5. Effect of suspension pH on the photoreduction of Mn^{2+} ions. HCOONa was present as the co-additive in each case (at 1 mM).

ordinate values of Mn^{2+} concentrations at zero time in each of the plots, directly reflect the amount initially adsorbed on the TiO_2 surface in the dark. For example, the "time zero" Mn^{2+} concentration for the sodium acetate co-additive case in Fig. 3 is ~125 μM, translating to an adsorbed amount of Mn^{2+} of ~75 μM.

Several trends emerge from the data in Fig. 3. Consistent with the energy band diagram in Fig. 1, direct reduction of Mn^{2+} by the photogenerated electrons in TiO_2 does not occur. Further, the alcohol co-additives exert no perceptible influence on the photoconversion of Mn^{2+}, i.e., these data mimic the control run (Fig. 3). In the presence of formate and oxalate ions, first-order kinetics are observed for Mn^{2+} removal from the suspensions—the formate being significantly more effective than oxalate. Sodium acetate exerts a very different effect. After a significant level of the initially added Mn^{2+} is adsorbed in the presence of this co-additive (see above and also Fig. 2), zero-order kinetics behavior is observed thereafter as the Mn^{2+} ions are photoreduced.

These results can be rationalized on the basis of a free radical-mediated indirect Mn^{2+} photoreduction route [8–14,20–24]. Thus, proton abstraction and/or initial oxidation of each of the anions ($HCOO^-$, CH_3COO^- and $C_2O_4^{2-}$) generate free radicals with considerable reducing power (Fig. 1). These radicals must be in close proximity to the interfacially bound Mn^{2+} ions resulting in the reduction of the latter and concomitant immobilization on the TiO_2 surface (see below for further evidence of this assertion). Note that the α-hydroxy methyl radical derived from methanol has insufficient reducing power (Fig. 1). The redox potential for the corresponding radical from isopropanol does lie higher (i.e., more negative) than the $Mn^{2+/0}$ redox potential (Fig. 1). The electron transfer kinetics from this radical to Mn^{2+} ions must then be sluggish. The ethanol case is interesting in that the corresponding redox potential involving its radical lies exactly at the level for the $Mn^{2+/0}$ couple (i.e., the thermodynamic driving force for electron transfer is 0). Once again, no reaction is observed here (Fig. 3).

If the above interfacial mechanistic picture is correct, then the amount of free radicals generated at the TiO_2 particle/solution interface ought to exert a pronounced effect on the Mn^{2+} photoconversion kinetics. The data contained in Fig. 4 for the formate co-additive show that this is indeed so. Co-additive levels were varied from 0.2 to 30 mM; the control run (0 mM formate) is also included here for comparison. Note that, to offset radical recombination (and other) losses, co-additive levels far in excess of stoichiometric requirements are needed to secure facile Mn^{2+} conversion. The definite plateau observed in Mn^{2+} conversion for the 0.2 mM formate case (Fig. 4) is diagnostic of a radical-limited kinetics regime.

3.3. Influence of suspension pH

Fig. 5 contains data on the influence of suspension pH. Sodium formate (1 mM) was used as the co-additive in this

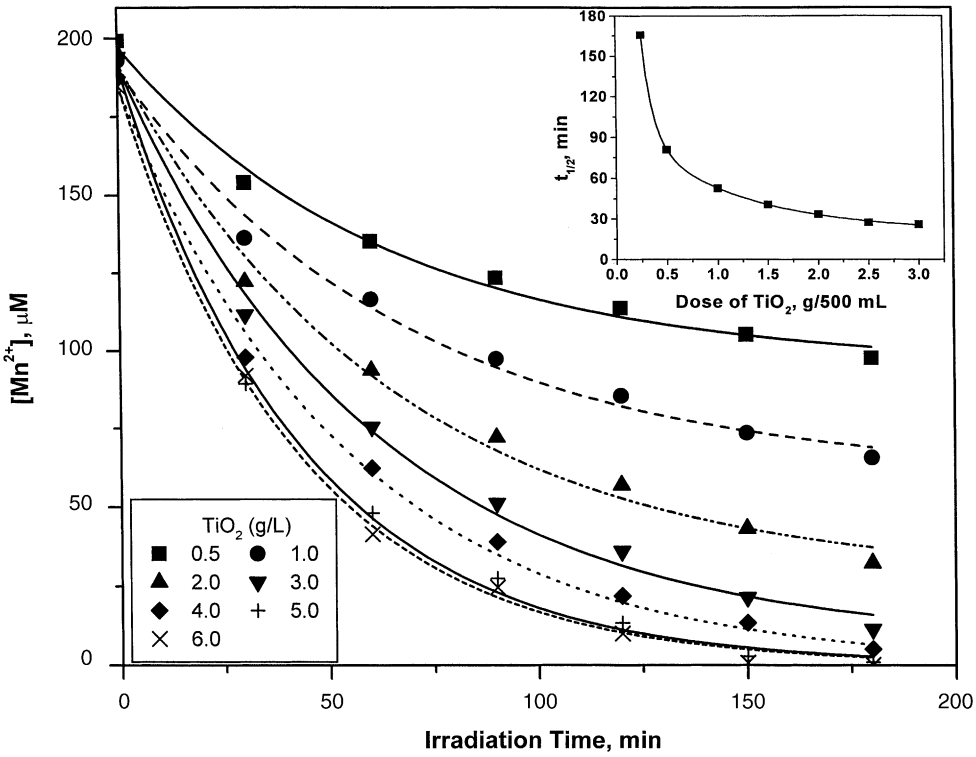

Fig. 6. Effect of TiO_2 solution dose on the photoreduction of Mn^{2+} ions. Other conditions as in Fig. 5. The insert shows the dependence of the photoreduction half-life ($t_{1/2}$) on the TiO_2 dose.

set of experiments. The co-additive level was *intentionally* kept at a low value (relative to the experiments in Fig. 3, for example) to clearly bring out the pH effect. Interestingly, when the suspension pH is below ~4, there is no photoreduction of Mn^{2+}. At a pH of 4.16, there is a ~1 h lag before observable conversion of Mn^{2+} is initiated. Note also that the initial (dark) adsorption of Mn^{2+} on the TiO_2 surface depends on the medium pH. At pH 4.0 or lower, there is negligible adsorption. Beyond pH 5.0, the Mn^{2+} adsorption increases up to the ~8.5 pH level studied (higher pH values are precluded by the tendency of Mn^{2+} to undergo base precipitation).

The adsorption trend can be rationalized on the basis of interfacial electrostatics; i.e., the point of zero charge (PZC) of TiO_2 is 5–6 [25–27]. Thus, at pHs lower than this value, the Mn^{2+} ions will be electrostatically repelled from the (positively charged) TiO_2 particle surface. At pHs higher than the PZC, the negatively charged TiO_2 surface will tend to bind the (positively charged) Mn^{2+} species. This simple interfacial picture also serves to delineate the two regimes pH $<$ 4 and pH $>\sim$ 5 separating the photoreactivity of Mn^{2+}. On the other hand, the "transition regime" (pH 4–5) deserves comment. The ionization equilibrium

$$HCOOH \Leftrightarrow H^+ + HCOO^-, \quad pK_a = 3.74 \qquad (1)$$

is shifted to the left in acidic media inhibiting the availability of the anionic species for initial photooxidation and free radical generation. In the pH 4.16 case, the lag time can be explained by a slow alteration (i.e., increase) of the *local* pH of the medium such that reaction (1) is progressively shifted to the right-hand side. One possible mechanism for this pH increase is proton reduction by the photogenerated electrons in TiO_2.

3.4. Influence of TiO_2 solution dose

Fig. 6 contains the relevant data again with 1 mM HCOONa as the co-additive. Note that at TiO_2 doses below ~1 g l^{-1}, we have a "photocatalyst-limited" reaction kinetics regime. On the other hand, there is a tendency towards saturation at TiO_2 doses higher than ~5 g l^{-1} as amplified in the figure insert. The photon utilization efficiency would clearly deteriorate at higher particle doses because of light-scattering and inner-filter effects [28]. A nominal TiO_2 dose of 2 g l^{-1} was thus deployed for all the experiments considered in Figs. 2–5 as a trade-off between acceptable optical losses vis à vis an adequate photocatalyst level (see insert, Fig. 6).

3.5. Photoreduction product identity

XPS analyses were inconclusive because of incipient oxidation of the initially deposited Mn species. The initially white TiO_2 suspensions during UV irradiation gradually

Table 1
FAAS assay of Cu^{2+} interaction with the Mn deposit on the TiO_2 surface

Condition	Mn^{2+} level in solution (μM)	
	Test 1	Test 2
Initial[a]	4.8	5.8
114 μM Cu^{2+} added[b]	94.5	–
132 μM Cu^{2+} added[b]	–	119

[a] After equilibration in the dark for 30 min with a TiO_2 suspension initially containing 200 μM $MnSO_4$ and 2 mM HCOONa, the UV lamp was turned on for 130 min.

[b] The UV lamp was turned off and 10 min elapsed before solution assay. The corresponding Cu^{2+} level in each case after this reaction period was 0 mM.

turned light gray consistent with the notion that the Mn^{2+} species were reduced to the elemental state. Thus, the following further set of experiments were undertaken to confirm this expectation.

First, the Mn^{2+} photoreduction was almost driven to completion in the TiO_2 suspension in the presence of 2 mM HCOONa as the co-additive. Then Cu^{2+} was added as the $CuSO_4{\cdot}5H_2O$ salt to the suspension after the UV lamp was turned off. After 10 min duration, sample aliquots were withdrawn for both Mn^{2+} and Cu^{2+} solution analyses by FAAS. The results are tabulated in Table 1 for two levels of addition of Cu^{2+} (114 and 132 μM, respectively).

Note that Mn^{2+} levels in the solution increased upon Cu^{2+} addition to the medium, and the level of Mn^{2+} (ejected from the TiO_2 surface) scaled with the amount of Cu^{2+} ions added. Clearly, galvanic oxidation of the photogenerated Mn^0 had occurred consistent with the scheme:

$$Mn^0 + Cu^{2+} \rightarrow Cu^0 + Mn^{2+} \quad (2)$$

Accordingly, the solution levels of Cu^{2+} also dropped to 0 as probed by FAAS. The thermodynamic driving force for reaction (2) is appreciable with the two redox potentials being: $E^0(Mn^{2+/0}) = -1.18\,V$ and $E^0(Cu^{2+/0}) = +0.34\,V$. If the immobilized Mn species had existed in other states (e.g., MnO and MnO_2), reaction (2) would not have occurred with the added Cu^{2+} species; i.e., the oxides would be electrochemically inert towards Cu^{2+}. In summation, the above data are consistent with our assignment of the photoreduced Mn^{2+} species as elemental Mn.

4. General discussion

Manganese joins the list of the other metal ions that we have recently studied: Zn^{2+} [8,9], Cd^{2+} [8] and Tl^+ [11] in that although all these species themselves are only weakly interactive with the TiO_2 surface, in the presence of "anchor" species such as $HCOO^-$ or CH_3COO^- ions, strong adsorption ensues in each case. It is also interesting that the more strongly adsorption-inducing species, namely acetate, provokes zero-order kinetics vis à vis the first-order kinetics observed for formate (Fig. 3).

It would appear from the results presented here (cf. Figs. 3 and 5) that stronger dark adsorption on the TiO_2 surface effectively translates to faster photoconversion. Both the contrasting influences of alcohol and acid anion co-additives (Fig. 3) and the trend at high versus low pH (Fig. 5) argue in favor of this picture. However, both the acetate co-additive case (Fig. 3) as well as recent data from our laboratory [29] suggest that this correlation must not be taken too far.

The other general conclusion that can be made from these data is that neither hot carrier effects nor significant carrier accumulation (with attendant Burstein band edge shifts, [30]) occur. Otherwise, direct reduction of Mn^{2+} by the photogenerated electrons in TiO_2 should have been observed. Thus, at least with the Degussa P-25 samples utilized here, localization of the photogenerated electrons (in surface traps) must be an efficient process and effectively mitigates against both hot carrier transfer and carrier accumulation in the conduction band. Further studies of adsorption and reaction pathways involving metal ions in TiO_2 suspensions (with and without UV irradiation) are in progress.

Acknowledgements

This research was funded in part by a grant from the US Department of Energy, Office of Basic Energy Sciences. The authors thank the reviewer for constructive criticisms of an earlier manuscript version.

References

[1] K. Rajeshwar, J. Appl. Electrochem. 25 (1995) 1067.
[2] A.L. Linsebigler, G. Lu, J.T. Yates Jr., Chem. Rev. 95 (1995) 735.
[3] A. Mills, S. Le Hunte, J. Photochem. Photobiol. A 108 (1997) 1.
[4] P. Pichat, in: G. Ertl, H. Knözinger, J. Weitkamp (Eds.), Handbook of Heterogeneous Photocatalysis, Vol. 4, VCH, Weinheim, 1997, p. 2111.
[5] D.M. Blake, Bibliography of Work on the Heterogeneous Photocatalytic Removal of Hazardous Compounds from Water and Air, NREL/TP-430-22197, January 1999.
[6] M.I. Litter, Appl. Catal. B: Environ. 23 (1999) 89.
[7] A. Fujishima, T.N. Rao, D.A. Tryk, J. Photochem. Photobiol. C 1 (2000) 1.
[8] C.R. Chenthamarakshan, K. Rajeshwar, Electrochem. Commun. 2 (2000) 527.
[9] C.R. Chenthamarakshan, H. Yang, Y. Ming, K. Rajeshwar, J. Electroanal. Chem. 494 (2000) 79.
[10] C.R. Chenthamarakshan, H. Yang, C.R. Savage, K. Rajeshwar, Res. Chem. Intermed. 25 (1999) 861.
[11] P. Kajitvichyanukul, C.R. Chenthamarakshan, K. Rajeshwar, S.R. Qasim, J. Electroanal. Chem. 519 (2002) 25.
[12] M.R. Prairie, L.R. Evans, B.M. Stange, S.L. Martinez, Environ. Sci. Technol. 27 (1993) 1776.
[13] T. Rajh, A.E. Ostafin, O.I. Micic, D.M. Tiede, M.C. Thurnauer, J. Phys. Chem. 100 (1996) 4538.
[14] M.C. Thurnauer, T. Rajh, D.M. Tiede, Acta Chem. Scand. 51 (1997) 610.

[15] A. Lozano, J. Garcia, X. Domenech, J. Casado, J. Photochem. Photobiol. A 69 (1992) 237.
[16] S. Kagaya, Y. Bitoh, K. Hasegawa, Chem. Lett. (1997) 155.
[17] Y. Matsumoto, M. Noguchi, T. Matsunaga, J. Phys. Chem. B 103 (1999) 7190.
[18] E.B. Sandell, H. Onishi, Photometric Determination of Traces of Metals, Part I, 4th Edition, Wiley/Interscience, New York, 1978, pp. 481–484.
[19] E.C. Butler, A.P. Davis, J. Photochem. Photobiol. A 70 (1993) 273.
[20] J. Cunningham, H. Zainal, J. Phys. Chem. 76 (1972) 2362.
[21] R. Baba, R. Konda, A. Fujishima, K. Honda, Chem. Lett. (1986) 1307.
[22] F. Forousan, T.C. Richards, A.J. Bard, J. Phys. Chem. 100 (1996) 18123.
[23] W.-Y. Lin, K. Rajeshwar, J. Electrochem. Soc. 144 (1997) 2751.
[24] V.J. Lilie, G. Beck, A. Henglein, Ber. Bunsenges. Phys. Chem. 75 (1971) 458.
[25] G.A. Parks, Chem. Rev. 65 (1965) 177.
[26] G.D. Parfitt, Prog. Surf. Membr. Sci. 11 (1976) 181.
[27] D.N. Furlong, D. Wells, H.F. Sasse, J. Phys. Chem. 89 (1985) 626.
[28] V. Augugliaro, V. Loddo, L. Palmisano, M. Schiavello, J. Catal. 153 (1995) 32.
[29] K. Rajeshwar, C.R. Chenthamarakshan, S. Goeringer, M. Djukic, Pure Appl. Chem. (in press).
[30] D. Fitzmaurice, Sol. Energy Mater. Sol. Cells 32 (1994) 289.